0026-895X/03/6405-1239–1250$7.00
MOLECULAR PHARMACOLOGY
Copyright © 2003 The American Society for Pharmacology and Experimental Therapeutics
Mol Pharmacol 64:1239–1250, 2003

Vol. 64, No. 5
2885/1105841
Printed in U.S.A.

Selective Interaction of ARF1 with the Carboxy-Terminal Tail Domain of the 5-HT_{2A} Receptor

DEREK N. ROBERTSON, MELANIE S. JOHNSON, LOUISE O. MOGGACH, PAMELA J. HOLLAND, EVE M. LUTZ, and RORY MITCHELL

MRC Membrane and Adapter Proteins Cooperative Group, Membrane Biology Interdisciplinary Research Group, University of Edinburgh, School of Biomedical and Clinical Laboratory Sciences, Hugh Robson Building, George Square, Edinburgh, Scotland, United Kingdom (D.N.R., M.S.J., L.O.M., P.J.H., R.M.); Department of Bioscience & Biotechnology, University of Strathclyde, Glasgow, Scotland, United Kingdom (E.M.L.)

Received August 6, 2003; accepted August 13, 2003

This article is available online at http://molpharm.aspetjournals.org

ABSTRACT

The 5-hydroxytryptamine 2A receptor (5-HT_{2A}R) is a member of the class I family of rhodopsin-related G protein-coupled receptors. The receptor is known to activate phospholipase C via the heterotrimeric G proteins $G_{q/11}$, but we showed previously that it can also signal through the phospholipase D (PLD) pathway in an ADP-ribosylation factor (ARF)-dependent manner that seems to be independent of $G_{q/11}$ (Mitchell et al., 1998). Both coimmunoprecipitation experiments and the effects of negative mutant ARF constructs on 5-HT_{2A}R-induced PLD activation here suggested that ARF1 may play a greater role than ARF6 in the function of this receptor. Furthermore, we demonstrated using glutathione *S*-transferase (GST)-fusion proteins of receptor domains that ARF1 and ARF6 bind to the third intracellular loop (i3) and the carboxy terminal tail (ct) of the 5-HT_{2A}R. The association of ARF1 with the ct domain of the receptor was stronger than its interaction with i3, or the interactions of ARF6 with either construct. Experiments using ARF mutants that are deficient in GTP loading, and the in vitro addition of GTPγS suggested that GTP loading enhances ARF1 binding to the receptor. The N376PxxY motif in the transmembrane 7 domain of the receptor (rather than a N376DPxxY mutant form) was shown to be essential for ARF-dependent PLD signaling and ARF1 coimmunoprecipitation. In GST-fusion proteins of the 5-HT_{2A}R ct domain, mutation of Asn376 to Asp also markedly reduced ARF1-HA binding, although additional motifs in the Asn376–Asn384 sequence and to a lesser extent elsewhere, seem also to contribute to the interaction.

The 5-hydroxytryptamine (5-HT) receptor superfamily represents a diverse group of receptors encompassing 14 different subtypes. All but one of them (5-HT_3) signal through G-protein-linked pathways. The different families of G protein-coupled receptors (GPCRs) for 5-HT transduce their signals via different heterotrimeric G proteins, with 5-HT_1 (and 5-HT_5) linking to $G_{i/o}$ effectors, 5-HT_2 signaling through $G_{q/11}$ to generate inositol trisphosphate and increase intracellular Ca^{2+} levels, and 5-HT_4, 5-HT_6, and 5-HT_7 all signaling through G_s to increase production of cyclic AMP (Raymond et al., 2001). The 5-HT_{2A}R is of particular interest because it has been implicated in a variety of major psychiatric disorders and in hallucinogenic drug action.

GPCR interactions with heterotrimeric G proteins often (but not exclusively) seem to involve the third intracellular loop (i3) (Wess et al., 1997). The i3 domains of various GPCRs have been shown to provide docking sites for heterotrimeric G protein $\beta\gamma$ subunits (Wu et al., 1998) as well as arrestins (Wu et al., 1997; Gelber et al., 1999), GPCR-kinases (Wu et al., 1998), and indeed ARFs (McCulloch et al., 2001; Ronaldson et al., 2002). In a number of GPCRs, other intracellular loops and ct domains have also been implicated in interactions with heterotrimeric G proteins and arrestins (Wu et al., 1997; Oakley et al., 2001). In the 5-HT_{2A}R, the i3 domain has been shown to be important for coupling to $G_{q/11}$ and the carboxyl terminal segment of the i3 loop in particular may

This work was supported by grants from the Medical Research Council (to R.M.) and the Wellcome Trust (to E.M.L.).

ABBREVIATIONS: 5-HT, 5-hydroxytryptamine, serotonin; 5-HT_{2A}R, 5-hydroxytryptamine 2A receptor; GPCR, G protein-coupled receptor; PLD, phospholipase D; ARF, ADP-ribosylation factor; i3, third intracellular loop domain; ct, carboxy-terminal tail domain; tm7, 7th transmembrane domain; sPrC, protein C epitope tag with signal sequence; HA, hemagglutinin epitope tag; BFA, brefeldin A; GST, glutathione *S*-transferase; NI IgG, nonimmune mouse IgG; PLC, phospholipase C; PCR, polymerase chain reaction; PrC, Protein C; bp, base pair(s); DMEM, Dulbecco's modified Eagle's medium; USG, Ultroser G; AEBSF, 4-(2-aminoethyl)-benzenesulfonylfluoride; PAGE, polyacrylamide gel electrophoresis; GTPγS, guanosine 5′-*O*-(3-thio)triphosphate; CHAPS, 3-[(3-cholamidopropyl)dimethylammonio]propanesulfonate; SBTI, soybean trypsin inhibitor; ECL, enhanced chemiluminescence; MEM, minimum essential medium; PEG, polyethylene glycol; GEF, GTP-exchange factor; BK, large-conductance potassium channel; PDZ, postsynaptic density 95/disc-large/ZO-1.

play a key role in the interaction (Roth et al., 1998). Arrestin isoforms bind to the i3 loop of the 5-HT_{2A}R as they do to i3 domains of the M_2 and M_3 muscarinic receptors, but show broader specificity in that both nonvisual and visual arrestins are bound (Wu et al., 1997; Gelber et al., 1999).

In addition to $G_{q/11}$-mediated phospholipase C (PLC) activation, the 5-HT_{2A}R can activate several other signaling pathways that may involve alternative direct coupling to the receptor. These include activation of phospholipase A_2 [which may be mediated by a coupling mechanism other than $G_{q/11}$ (Berg et al., 1998)], activation of tyrosine phosphorylation [correlating with evidence for association of the tyrosine kinase Jak2 with the ct domain (Guillet-Deniau et al., 1997)] and ARF-dependent activation of phospholipase D (PLD) (Mitchell et al., 1998).

A specific conserved motif, NPxxY, which is found at the junction of the tm7 and ct domains in a number of rhodopsin family GPCRs, has been implicated as a determinant of ARF-receptor interactions and ARF-mediated signaling, because native receptors with an alternative DPxxY motif, or Asn-to-Asp mutant receptors, show selective defects in this pathway (Mitchell et al., 1998, 2003). However, it has not been clear whether this motif might be accessible as a direct docking site or it instead regulates access to a distinct site.

The two main classes of cellular ARFs are exemplified by ARF1 and ARF6, which are thought to have characteristically distinct subcellular distributions. In many cells, ARF1 is cytosolic or associated with Golgi membranes, whereas ARF6 may be substantially associated with plasma membrane and play a role in regulating endocytosis (D'Souza-Schorey et al., 1995; Peters et al., 1995; Cavenagh et al., 1996). Nevertheless, GTP loading and GPCR activation can cause translocation of ARFs to Golgi and other membranes, and we have shown marked translocation of ARF1 to the plasma membrane after activation of the M_3 muscarinic receptor (Mitchell et al., 2003) and the 5-HT_{2A}R (M. Johnson and R. Mitchell, unpublished observations). Thus both ARF1 and ARF6 are potentially available for interaction with plasma membrane GPCRs after agonist stimulation.

In this study, we have addressed the role of ARF1 and ARF6 in 5-HT_{2A}R-mediated PLD signaling, demonstrated coimmunoprecipitation of ARF1 (and to a lesser extent ARF6) with the receptor, and gone on to characterize the docking of ARFs to GST fusion proteins of receptor i3 and ct domains.

Materials and Methods

Preparation of sPrC-Tagged 5-HT_{2A} Receptor and sPrC-Tagged N376D-5-HT_{2A} Mutant Receptor Constructs. The wild-type human 5-HT_{2A}R cDNA (SCS93) and N376D-5-HT_{2A}R mutant cDNA (SCS103), cloned into pcDNA1-amp (Invitrogen, Paisley, UK), were kindly provided by Stuart Sealfon (Mount Sinai School of Medicine, New York, NY). To create an amino terminal epitope-tagged receptor, SCS93 was PCR-amplified with the synthetic oligonucleotide primers [5′-GAAGATCAGGTAGATCCACGGTTAATC-GATGGTAAGGCCATGGATATTCTTTGTGAAG-3′] encoding the 12-amino acid Protein C tag (PrC) epitope (EDQVDPRLIDGK) and the reverse primer named 5HT_{2A}.rp, [5′-GAATTCTCACACA-CAGCTCACCTTTTCATT-3′] using the Herculase-enhanced DNA polymerase (Stratagene Europe, Amsterdam, NL). The resulting PCR product was checked by agarose gel electrophoresis and extracted with Wizard PCR clean-up resin (Promega, Southampton, UK) before amplifying with the primer [5′-GCCACCATGAAGAC-GATCATCGCCCTGAGCTACATCTTCTGC-CTGGTATTCGCCGAAGATCAGGTAGATCCAC-3′] encoding a modified influenza hemagglutinin signal sequence and 5HT_{2A}.rp. The 1.4-kilobase fragment was purified by agarose gel electrophoresis and Qiaex II (QIAGEN Ltd.,Crawley, UK), then subcloned into TOPO TA cloning vector (Invitrogen). The sPrC-5-HT_{2A} insert was checked by sequencing. For expression studies, the sPrC-tagged wild-type receptor was constructed by subcloning the 200-bp *Eco*RI/*Sal*I fragment from sPrC-5-HT_{2A} cDNA and the 1.5-kilobase *Sal*I/*Xba*I fragment from SCS93 into the *Eco*RI/*Xba*I site of pcDNA3 (Invitrogen). The sPrC-tagged (N376D) mutant receptor was constructed by subcloning the 450-bp *Eco*RI/*Pst*I fragment from sPrC-5-HT_{2A} cDNA and the 1.3-kilobase *Pst*I/*Xba*I fragment from SCS103 into the *Eco*RI/*Xba*I site of pcDNA3 (Invitrogen).

Construction of 5-HT_{2A} Receptor Intracellular Loop 3 and Carboxy Terminal Tail GST-Fusion Proteins. The human 5-HT_{2A}R intracellular loop 3 (Ile258–Gly326) was PCR-amplified from SCS93 with primer pair [5′-GGGTGATCAAGTCACTTCA-GAAAGAAGCTAC-3′] and [5′-CGGAATTCTAGCCCAGCACCTTG-CATGCTTTTGCTCATTGCT-3′], and the resulting 200-bp PCR product was purified, digested with *Bcl*I/*Eco*RI, and subcloned into the *Bam*HI/*Eco*RI sites of pGEX-3X (Amersham Biosciences, Little Chalfont, UK). The 347-bp *Hinc*II fragment encoding the human 5-HT_{2A}R carboxy-terminal tail and including the NPLVY motif (Asn376-Val471) was subcloned into the modified (with Mung bean nuclease; Stratagene, La Jolla, CA) *Bam*HI site of pGEX-2T. The sequences encoding the carboxy-terminal tail amino acids (Lys385–Val471) were PCR-amplified from SCS93 using primer pair Bh2ARCT.KTYRS [5′-CGGGATCCAAAGACCTATAGGTCAGC-CTTTTCACG-3′] and h2ARCT.rp [5′-CAACTCAATTGTCACACA-CAGCTCACCTTTTCATT-3′], and the mutant (N376D-Val471) carboxyl tail was PCR-amplified from SCS103 with primer pair h2ARCT.DPLVY [5′-CGGGATCCAGACCCACTAGTCTACA-CACTGTTCAA-3′] and h2ARCT.rp using *Taq* polymerase (Promega) and the resulting PCR products purified by Wizard cDNA clean-up resin (Promega), digested with *Bam*HI/*Mfe*I and subcloned into the *Bam*HI/*Eco*RI sites of pGEX-2T. The *Bam*HI sites then were modified with Mung bean nuclease. Cloned inserts were checked by sequence analysis.

Transient Transfections of Cells. COS-7 cells were grown to 60% confluence in Dulbecco's modified Eagle's medium (DMEM; Invitrogen) containing 10% normal calf serum and 100 units/ml penicillin and 100 μg/ml streptomycin. Before transfection, medium was changed for DMEM containing 2% Ultroser G (USG; Invitrogen) instead of serum. The cells were then transfected with combinations of the cDNAs for sPrC-5-HT_{2A}R, ARF1-V5-His_6 (Invitrogen), ARF1 and ARF6 tagged with the hemagglutinin epitope (HA) at the carboxyl terminal, or the dominant-negative mutants T31N-ARF1-HA and T27N-ARF6-HA (Peters et al., 1995) (kindly provided by Julie Donaldson, National Institutes of Health). All transfections (normally at a ratio of 4 μg of receptor construct cDNA to 1 μg of ARF construct cDNA per 75-cm^2 flask) were carried out using FuGENE-6 reagent (Roche Diagnostics Ltd, Lewes, UK) according to the manufacturer's guidelines, and appropriate substitutions of empty vectors were made in control samples. Transfected cells were used 72 h after transfection.

Preparation of ARF-Enriched Extracts. COS-7 cells transfected with various ARF-HA constructs were washed with 10 ml of Earle's balanced salt solution (Invitrogen) before being scraped into ice-cold extraction buffer [2 ml/175-cm^2 flask, 2 μg/ml aprotinin, 1 mM 4-(2-aminoethyl)-benzenesulfonylfluoride (AEBSF) (Alexis Biochemicals, San Diego, CA), 1 mM dithiothreitol, 1 mM pepstatin, 1 mM sodium orthovanadate, 1 mM NaF, 50 μg/ml soybean trypsin inhibitor (SBTI) in PBS]. All chemicals were from Sigma Chemical Co. (Poole, Dorset, UK) unless otherwise indicated. The cells were then homogenized [Ystral homogenizer (Scientific Industries Intl. UK Ltd, Loughborough, UK) setting 3, 15 s] before being centrifuged

at 12,000*g* for 20 min at 4°C. The supernatant was aliquoted and stored at −40°C.

Purification of ARF1-V5-His$_6$ on Cobalt Affinity Resin. COS-7 cells were transfected with an expression plasmid encoding ARF1-V5-His$_6$, and enriched cytosol was isolated as described above. The cytosolic extracts over-expressing the ARF1-V5-His$_6$ were then incubated with 'Talon' cobalt affinity resin (BD Biosciences Clontech, Palo Alto, CA) that had been pre-equilibrated with wash buffer (10 mM sodium phosphate, 60 mM NaCl, pH 7.0), for 1 h at 4°C. The resin was washed thoroughly with extraction/wash buffer (additionally containing 5 mM imidazole) before being eluted using elution buffer (additionally containing 300 mM imidazole) according to the manufacturer's instructions. The purified ARF1-V5-His$_6$ was then concentrated using Centriplus centrifugal filters (YM-3; Millipore, Bedford, MA) according to the manufacturer's instructions. The amount of protein present was verified by colorimetric measurement using Coomassie protein reagent (Perbio Science UK Ltd., Tattenhall, Cheshire, UK). The percentage purity of the harvested protein purity was then assessed by staining with high sensitivity Colloidal Coomassie (Simply Blue Safe stain; Invitrogen) on an SDS-PAGE gel, identifying the correct band by Western blotting using mouse monoclonal V5-tag antibody (Invitrogen). Standard curves were produced from the purified ARF1-V5-His$_6$ (linear range from 0.4–7.2 ng ARF1-V5-His$_6$ per well). These were coprocessed with experimental samples of cytosolic inputs and of proteins associating with the receptor in either coimmunoprecipitation or GST-fusion protein experiments, enabling us to assess the amounts of ARF1-V5-His$_6$ present.

Expression of GST Proteins. GST-5-HT$_{2A}$i3 and GST-5-HT$_{2A}$ct constructs, in the pGEX-3X and pGEX-2T vectors, as well as a control GST fusion protein of the STREX insert of the large conductance Ca^{2+}- and voltage-activated K^+ (BK) channel, in the pGEX-5 × 1 vector (kindly supplied by Mike Shipston, University of Edinburgh) were expressed in BL21-RIL bacterial cells, grown in standard 2× yeast extract/tryptone/NaCl medium with 2% glucose. When the cells had reached an A_{600} of 0.6 to 0.8 units/ml, expression of the fusion proteins was induced by the addition of 0.1 mM isopropyl-β-D-thiogalactoside for 3 h at 37°C. Cells were harvested by centrifugation then lysed with BugBuster reagent (Merck Biosciences, Beeston, Nottingham, UK) for 10 min and again centrifuged. The supernatant, containing the GST fusion proteins, was added to glutathione-Sepharose beads (Amersham Biosciences). The beads were incubated with the bacterial supernatant for 20 min at room temperature to allow binding of the GST fusion proteins to the beads. The matrix formed was then washed extensively with PBS and used immediately.

In Vitro Protein Interaction Assays. Cellular extracts enriched in the various HA-tagged ARF constructs were incubated with GST fusion proteins bound to glutathione-Sepharose beads (Amersham Biosciences) in 250 μl of buffer A (20 mM Tris-HCl, pH 7.5, 0.6 mM EDTA, 1 mM dithiothreitol, 70 mM NaCl, and 0.05% Tween 80) for 90 min at 4°C, with rolling. In some experiments, GTPγS (100 μM) was added to the incubations. The beads were washed four times in buffer A and then the retained proteins were removed from the beads with 2× Laemmli buffer (2% SDS, 5% mercaptoethanol, 20 mM Tris-HCl, pH 7.4) before SDS-PAGE and immunoblotting (see below). Input levels of fusion proteins (monitored by GST immunoreactivity) were carefully balanced to ensure comparability between samples. Protein interaction assays using ARF1-V5-His$_6$ were carried out in an identical manner, except that increased amounts of bacterial cytosol containing GST construct was added to the glutathione-Sepharose beads (~2×).

Coimmunoprecipitation of sPrC-5-HT$_{2A}$ Receptor and ARF1/6-HA. Transfected COS-7 cells were incubated in medium alone (no serum or USG) for 4 h before being exposed to 5-HT (10 nM–10 μM) and/or brefeldin A (BFA, 100 μM). Cells were washed once in Hank's balanced salt solution (HBSS; Invitrogen) before the addition of 1 ml/75-cm^2 flask of immunoprecipitation buffer (HEPES 20 mM, pH 7.5, NaCl 150 mM, 1% CHAPS, 0.5% sodium deoxycholate, 2 μg/ml aprotinin, 4 μg/ml leupeptin, 1 mM AEBSF, 2 μg/ml pepstatin, 1 mM sodium orthovanadate, 1 mM sodium fluoride, 5 mM sodium molybdate, and 50 μg/ml SBTI) with 5-HT if it had been used in the initial stimulation. Extraction was carried out on ice for 40 min with occasional agitation. Solubilized cellular extracts were centrifuged at 12,000*g* for 15 min at 4°C to remove particulate material. One ml of supernatant was precleared with 20 μl of protein G-Sepharose 4B fast flow (50% suspension in immunoprecipitation buffer) for 45 min at 4°C. After centrifugation (to pellet the beads), the supernatant was added to a tube containing either mouse monoclonal (Ca^{2+}-dependent) PrC-tag antibody (clone HPC4, 4 μg/ml; Roche) or control, nonimmune mouse IgG, 4 μg/ml; Sigma) with 40 μl/ml protein G-Sepharose suspension and 1 mM $CaCl_2$. Samples were incubated with rolling, at 4°C overnight. In the standard procedure, the beads were pelleted, washed twice in immunoprecipitation buffer before 40 μl of 2× Laemmli buffer containing 5 mM EGTA was added per sample equivalent to 1 ml of original supernatant. In some experiments, the receptor complex was removed from the PrC antibody-protein G-Sepharose beads by incubation in 50 mM Tris and 2 mM EGTA, pH 7.5, for 30 min at room temperature. The supernatant was removed and SDS and mercaptoethanol added equivalent to 2× Laemmli buffer.

Western Blots. Western blots were carried out on samples from immunoprecipitation and GST fusion protein interaction assays. Either 20% or 12.5% precast homogeneous PhastGels (Amersham Biosciences) were used. SDS-PAGE and electroblotting onto polyvinylidene difluoride membranes (Immobilon-P^{SQ}, Millipore, Watford, UK) were performed on a PhastSystem apparatus (Amersham Biosciences). The detection antibodies were rabbit polyclonal anti-HA (Autogen Bioclear, Calne, Wilts, UK), goat polyclonal anti-GST (Amersham Biosciences) and mouse monoclonal anti-PrC (Roche) followed by preabsorbed secondary antibodies conjugated to horseradish peroxidase (Chemicon Intl. Ltd., Harrow, UK). Visualization of antibody bands was by Luminol (New England Biolabs, Hitchin, UK), and blots were exposed to ECL film (Amersham Biosciences). Densitometric analysis of ECL images from Western blots was carried out using the ScanAnalysis program (Biosoft, Cambridge, UK). Immunoprecipitation samples were also run on larger gels on the NuPAGE SureLock mini-cell system (Invitrogen) under reducing conditions, with 10% homogenous Bis-Tris gels and then blotted on the same system according to the manufacturer's instructions.

PLD Assays. Transfected cells in 12-well plates were deprived of USG by transferring to DMEM for 18 h, during which time they were labeled with [^{3}H]palmitate (1.5 μCi/well; PerkinElmer Biosciences, Hounslow, UK). After washing with minimal essential medium containing HEPES (25 mM, pH 7.5) and 0.5% fatty acid-free bovine serum albumin, cells were preincubated for 20 min in similar medium with or without BFA, before addition of butan-1-ol (30 mM) and various concentrations of 5-HT for a further 30 min. The vehicle for BFA (dimethylformamide at 0.2%) was added to control wells and has been shown previously to have no detectable effect on signaling responses. Reactions were terminated by removal of medium and addition of 0.5 ml ice-cold methanol to each well. Phospholipids were extracted and [^{3}H]phosphatidyl butanol was separated on Whatman LK5D thin-layer chromatography plates (Whatman, Maidstone, Kent, UK) as described previously (Mitchell et al., 2003).

PLC Assays. Transfected cells in 12-well plates were deprived of USG by transferring to Earle's balanced salt solution containing 10 mM HEPES, pH 7.5, and 0.18% glucose for 18 h, during which time they were labeled with [^{3}H]inositol (0.75 μCi/well; PerkinElmer Biosciences). The medium was changed for Earle's balanced salt solution containing 10 mM HEPES, 0.18% glucose, and 0.2% bovine serum albumin and washed once. Cells were preincubated for 20 min with 10 mM LiCl (and BFA where required) before being incubated for 30 min with various concentrations of 5-HT with or without BFA. Reactions were terminated by the removal of medium and the addition of 1 ml of ice-cold 10 mM formic acid (Sealfon et al., 1995) and

the cells were left on ice for at least an hour to ensure lysis. Inositol phosphates ([^{3}H]InsP) were separated by anion exchange chromatography as described previously (Mitchell et al., 2003).

[^{3}H]Ketanserin Binding. Assessment of PrC-5-HT$_{2A}$ receptor expression in the transfected COS-7 cells was by homologous displacement of [^{3}H]ketanserin binding (specific activity, 88.0 Ci/mmol; PerkinElmer Life Sciences). After removal of USG from the culture medium for the last 4 h, cell membranes were prepared by harvesting the cells into ice-cold ketanserin binding buffer (50 mM Tris, 5 mM $MgCl_2$, and 1 mM EGTA, pH 7.2) and disrupted with an Ystral homogenizer. Membranes were washed twice in buffer, centrifuging each time at 12,000*g*, 30 min, 4°C. Finally the membranes were suspended in buffer at ~200 μg/ml protein. Membranes were incubated for 60 min at 37°C with 0.8 nM [^{3}H]ketanserin and either no other drug, increasing concentrations of unlabeled ketanserin, or 10 μM mianserin to determine nonspecific binding. At the end of the assay, binding was stopped by addition of ice-cold buffer, the membranes were pelleted by centrifugation (10 min at 12,000*g*) and the supernatant was aspirated. Bound radioactivity was determined by liquid scintillation counting. The homologous displacement curves were fitted to a Hill model using nonlinear curve fitting program, Fig-P (Biosoft, Cambridge, UK). This allowed measurement of K_D and number of binding sites. For experiments to determine receptor binding where cell membranes were solubilized in immunoprecipitation buffer, the lysate was first treated with polyethylene glycol-8000 (PEG; final concentration, 15%) to precipitate solubilized proteins, including PrC-5-HT$_{2A}$ receptor, and washed, again precipitating with PEG before trituration of the pellet in ketanserin binding buffer for the assay. Additionally, PEG was used to terminate the assay, and nonsolubilized membranes included in the experiments as controls were treated in the same way.

When membranes were treated with solubilization buffer, the total amount of specific [^{3}H]ketanserin binding that was recovered from the supernatant plus residual membrane fractions was much less than the input levels of binding in untreated membranes (approximately 15%). It is not clear to what extent this was caused by deleterious effects of detergent/PEG exposure on the ligand binding site or by inefficient capture of solubilized receptor. However, some loss of ligand binding capacity is likely to result during these procedures. It therefore seems likely that the amount of receptor still detectable by ligand binding after extraction represents an underestimate of the amount of receptor protein actually solubilized. Nevertheless, some 97% of the [^{3}H]ketanserin binding that could be recovered was found in the solubilized fraction. When this fraction was immunoprecipitated with PrC-tag antibody, the proportion of solubilized specific binding that became associated with the protein G beads rather than remaining in the supernatant was 70 ± 18%.

[^{3}H]Ketanserin Binding to Coimmunoprecipitates. Cells transfected with wild-type or N376D mutant sPrC-5-HT$_{2A}$ constructs and wild-type ARF1-HA were transferred to USG-free DMEM for 16 h before assay. After washing in PBS at 37°C, and incubation with 5-HT (1 μM, 5 min) in some cases, cells were scraped into ice-cold buffer (PBS, 10% glycerol, 2 μg/ml aprotinin, 4 μg/ml leupeptin, 1 mM AEBSF, 2 μg/ml pepstatin A, 50 μg/ml SBTI, 1 mM sodium orthovanadate, and 1 mM sodium fluoride) and homogenized using an Ystral homogenizer. Nuclei and debris were removed by centrifugation at 1000*g* for 8 min before the supernatant was centrifuged (12,000*g* for 30 min) to obtain a membrane fragment pellet. The pellet was washed once before trituration in the above buffer containing 1% CHAPS and 0.75% deoxycholate and rolling for 30 min at 4°C. Samples were precleared with protein G-Sepharose and then centrifuged (12,000*g*; 30 min) to obtain the solubilized extracts used for immunoprecipitation. Samples were incubated with 2 μg/ml mouse monoclonal anti-HA tag (clone 12CA5) or nonimmune mouse IgG for 90 min at 4°C and then immune complexes were collected by incubation with protein G-Sepharose for 45 min at 4°C. The pellets from centrifugation at 12,000*g* for 10 min were washed once in solubilizing buffer and then resuspended in [^{3}H]ketanserin binding buffer (see above) that additionally contained 10% glycerol. Ligand binding was assayed as described above. Incubations (250 μl) were stopped by the addition at 4°C of 100 μl of 0.05% bovine γ-globulin in PBS and 1 ml of 30% PEG in PBS. After 15 min on ice, samples were centrifuged at 12,000*g* for 20 min, the supernatant was aspirated, and the tube tips were removed for liquid scintillation counting.

Results

Figure 1 illustrates functional signaling responses of the sPrC-5-HT$_{2A}$R expressed in COS-7 cells. [^{3}H]Ketanserin binding experiments indicated that the sPrC-5-HT$_{2A}$R was expressed in COS-7 cell membranes at a mean level of 0.84 ± 0.04 pmol/mg of total protein, with an IC_{50} for homologous displacement of 4.8 ± 0.4 nM. The receptor produced robust PLC and PLD activation responses to 5-HT stimulation that were similar to the untagged receptor (Sealfon et al., 1995; Mitchell et al., 1998) but with slightly greater potency; the EC_{50} values for PLC and PLD responses were 5.0 ± 2.2 and 6.8 ± 1.9 nM, respectively (Fig. 1, A and B). The EC_{50} value for PLC activation by the untagged receptor in similar experiments was found to be 28 ± 2 nM (R. Mitchell and M. Johnson, unpublished observations) and 22 ± 5 nM (Sealfon et al., 1995). The effects of cotransfection of ARF mutants were investigated on 5-HT-induced signaling events mediated by the sPrC-5-HT$_{2A}$R expressed in COS-7 cells. PLC activation was unaffected by cotransfection of either T31N-ARF1-HA or T27N-ARF6-HA; mutant constructs of the ARF isoforms that have a dysfunctional GTP binding domain (Peters et al., 1995) (Fig. 1A). However, T31N-ARF1-HA, but not T27N-ARF6-HA, significantly inhibited 5-HT$_{2A}$R-mediated PLD activation (Fig. 1B). Figure 1C shows the inhibitory effect of BFA [a blocker of the BIG1/2 class of ARF GTP-exchange factor (GEF) (Morinaga et al., 1999)] on the PLD response of the 5-HT$_{2A}$ receptor. When only the receptor was expressed, BFA caused a concentration-dependent inhibition of 5-HT–induced PLD activation, with significant inhibition at 50 μM and above. In cells additionally expressing T27N-ARF6-HA, BFA was also inhibitory throughout a similar concentration range. However, in cells expressing T31N-ARF1-HA, the residual 5-HT–induced PLD response became insensitive to BFA. The PLC response of the 5-HT$_{2A}$R was unaffected by BFA (data not shown).

To investigate whether a physical interaction of either ARF1 or ARF6 with the receptor occurs upon activation, we looked for coimmunoprecipitation of HA-tagged ARF isoforms with the sPrC-5-HT$_{2A}$R (Fig. 2). When nonimmune mouse IgG (NI IgG) was substituted for the PrC-tag antibody in the immunoprecipitation, minimal levels of either ARF1-HA or ARF6-HA immunoreactivity could be detected in the pulldown assays. Significant levels of ARF1-HA (and to a much lesser extent, ARF6-HA) seemed to be specifically associated with the PrC-tag antibody pulldown assays of the sPrC-5-HT$_{2A}$R, even under basal conditions (Fig. 2A). Densitometric analysis indicated that basal levels of ARF1-HA coimmunoprecipitated were increased on average 3.32 ± 1.58-fold (n = 5) over nonspecific, as determined with NI IgG. The corresponding value for ARF6-HA was lower, a 0.32 ± 0.05-fold (n = 3) increase over nonspecific. Relative densitometric values of anti-HA tag blots for coimmunoprecipitated ARF1-HA as a percentage of the input of total expressed ARF1-HA were 0.13 ± 0.03% in unstimulated

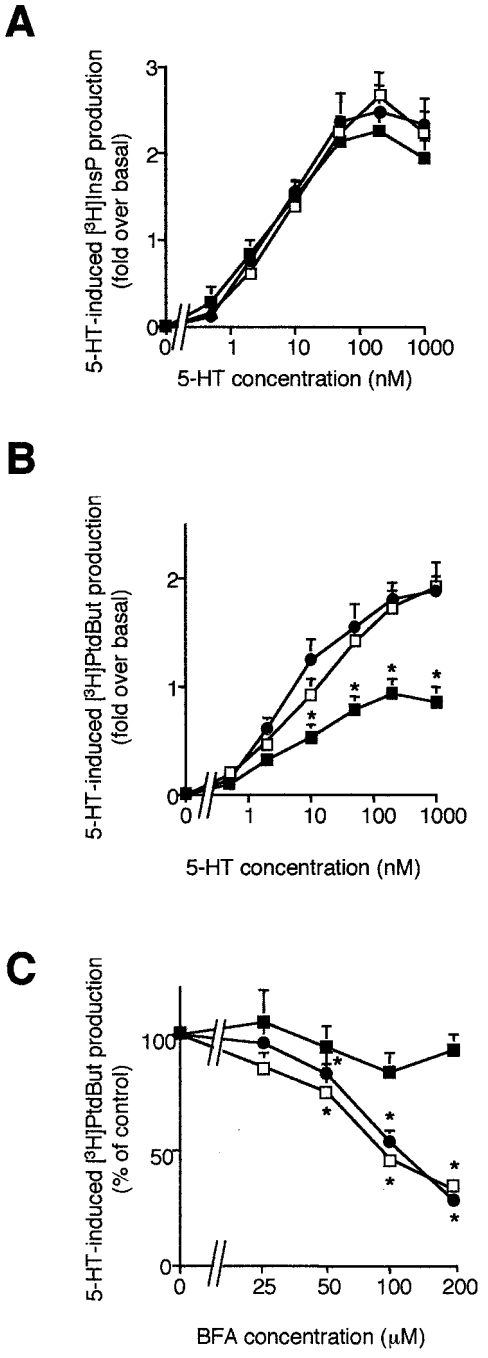

Fig. 1. Effects of mutant ARF1 and ARF6 constructs on signaling responses of the sPrC-5-HT$_{2A}$ receptor. COS-7 cells were cotransfected with the sPrC-5-HT$_{2A}$R together with either empty vector (●), T31N-ARF1-HA (■), or T27N-ARF6-HA (□). Values are means ± S.E.M., n = 6–8. A, concentration-dependence of 5-HT-induced PLC activation; there was no discernible effect of the negative mutant ARFs on this response. B, concentration-dependence of 5-HT-induced PLD activation. The addition of T27N-ARF6-HA had no significant effect on the ability of the 5-HT$_{2A}$R to activate PLD, whereas the presence of T31N-ARF1-HA significantly attenuated the PLD response to 5-HT concentrations of 10 nM and above (*, $p < 0.05$ by Wilcoxon test). C, BFA sensitivity of the 1 μM 5-HT-induced 5-HT$_{2A}$R PLD response and a concentration-dependent inhibition that was statistically significant (*, $p < 0.05$, Wilcoxon test) for BFA concentrations of 50 μM and above in control and T27N-ARF6-HA samples. Cotransfection of T27N-ARF6-HA had no discernible effect on BFA sensitivity compared with control, whereas the PLD response in the presence of T31N-ARF1-HA was no longer significantly inhibited by BFA.

samples compared with 0.21 ± 0.03% after 5-HT (1 μM, 5 min). Equivalent values for ARF6-HA were 0.053 ± 0.010% and 0.067 ± 0.008%, respectively. Although coimmunoprecipitation of both isoforms of ARF with the receptor seemed to be increased by addition of 5-HT (mean increase to 1.61- and 1.26-fold of control, respectively), only the effect on ARF1-HA was statistically significant ($p < 0.05$, Wilcoxon test, $n = 5$ in each case) These values are useful for relative comparisons but do not faithfully reflect the fraction of ARF1/6-HA within an individual cell that is associated with sPrC-5-HT$_{2A}$ receptor, because we know from dual label confocal immunofluorescence experiments (data not shown) that a subpopulation of the COS-7 cells expressing ARF constructs fail to express detectable levels of receptor. When the input level of sPrC-5-HT$_{2A}$R was varied by substituting pcDNA3 for part of the receptor cDNA in the transfection (while keeping the ARF1-HA plasmid concentration constant), less ARF1-HA was coimmunoprecipitated, in proportion to the level of receptor expression as monitored by specific [^{3}H]ketanserin binding (Fig. 2B).

An attempt to quantify the amount of ARF1 specifically coimmunoprecipitating with the receptor was made by cotransfection of an ARF1-V5-His$_6$ construct, the binding of which was then monitored as anti-V5 tag immunoreactivity. Densitometric measurements of ARF1-V5-His$_6$ coimmunoprecipitated with the receptor by PrC tag antibody (or NI IgG control), as well as input levels of ARF1-V5-His$_6$ in cell lysates, were compared with a coprocessed standard curve of anti-V5 tag immunoreactivity prepared using ARF1-V5-His$_6$ protein, purified on a Co^{2+} affinity column. The protein content of the purified ARF1-V5-His$_6$ standard was determined, allowing estimation of the absolute amount of ARF1-V5-His$_6$ that was specifically coimmunoprecipitated in the PrC-tag antibody pulldown assays. Under basal conditions, this was calculated as 11.1 ± 1.0 ng of ARF1-V5-His$_6$ protein from one 175-cm^2 flask. Because essentially all transfected COS-7 cells expressing detectable levels of sPrC-5-HT$_{2A}$R also express ARF constructs, comparison of the amount of coimmunoprecipitated ARF with the B_{max} for [^{3}H]ketanserin binding in equivalent samples allows an estimate of the mean proportion of sPrC-5-HT$_{2A}$Rs that were bound to ARF1-V5-His$_6$. Under basal conditions, this was calculated as 23% of the total; under 5-HT–stimulated conditions, this would be predicted to increase to 37% (1.61-fold of basal association). However, as pointed out above, it is not possible to use this approach to reliably estimate the proportion of expressed ARF construct that is associated with receptor.

The effect of 5-HT on coimmunoprecipitation of ARF1-HA with the sPrC-5-HT$_{2A}$R was investigated further (Fig. 3). Nonimmune mouse IgG controls for 5-HT–stimulated samples gave results similar to those of unstimulated NI IgG controls (data not shown). The time course of 1 μM 5-HT-induced changes in coimmunoprecipitation of ARF1-HA with sPrC-5-HT$_{2A}$R showed a clear increase in association from 2 min, a peak around 5 min, and then a gradual decline (although levels seemed to remain above basal for as long as 2 h) (Fig. 3A). The concentration dependence of the effect of 5-HT (10-min incubation) is shown by the insert in Fig. 3A, reaching a maximum by approximately 1 μM 5-HT. Figure 3B shows that the 5-HT-induced increase in ARF1-HA coimmunoprecipitation with the sPrC-5-HT$_{2A}$R was reduced to basal levels by the ARF-GEF inhibitor, BFA (100 μM) (Fig. 3B). As before, the concentration of ARF1-HA present in the

lysate was very similar between the different conditions (as shown in Fig. 3B, middle), and the amount of receptor immunoprecipitated (Fig. 3B, top) was also even. These observations using immunoprecipitation of the sPrC-5-HT_{2A}R indicate that ARF1, and to a lesser extent ARF6, shows a physical association with the receptor that can be increased in the presence of 5-HT, correlating with the functional studies on PLD activation.

To examine the receptor-ARF interaction in more detail, we generated GST fusion protein constructs of the intracellular loop 3 (i3; Ile258–Gly326) and carboxy-terminal tail (ct; Asn376-Val471) of the 5-HT_{2A}R, and investigated their ability to bind ARF1-HA and ARF6-HA in vitro. Figure 4 is a schematic representation of the 5-HT_{2A}R showing the amino acid sequences used for these GST constructs. GST-fusion protein constructs of the i3 and ct domains of the 5-HT_{2A}R, or the STREX exon of the BK channel as a control, were attached to glutathione Sepharose beads and used in in vitro interaction assays at equivalent input levels [as estimated by GST immunoreactivity (Fig. 5A)]. The input levels of ARF1-HA and ARF6-HA or the negative mutant constructs, deficient in GTP binding, T31N-ARF1-HA and T27N-ARF6-HA, were also balanced for HA-immunoreactivity (Fig. 5A). Figure 5B compares ARF1-HA and ARF6-HA interaction with the constructs. ARF1-HA showed much greater relative binding to the ct domain of the 5-HT_{2A}R than to the BK channel construct or the i3 domain of the 5-HT_{2A}R. ARF6-HA showed a much lower level of binding to the 5-HT_{2A}ct construct and little interaction with the 5-HT_{2A}i3 or BK constructs. Figure 5C shows the binding profiles for the functionally negative mutants of ARF1 and ARF6, T31N-ARF1-HA and T27N-ARF6-HA. The binding of T31N-ARF1-HA to the 5-HT_{2A}ct construct was greatly reduced compared with that of the ARF1-HA wild type, whereas the low background levels of T31N-ARF1-HA binding to 5-HT_{2A}i3 and BK channel constructs were similar to those seen with wild-type ARF1-HA. T27N-ARF6-HA showed a low level of binding to the 5-HT_{2A}ct construct that seemed to be similar to that of the ARF6-HA wild type. The apparently slightly higher levels of T27N-ARF6-HA binding compared with the wild type in the experiment displayed correspond to its somewhat higher input level. GTPγS facilitated the interaction of submaximal levels of ARF1-HA with the 5-HT_{2A}ct construct and also seemed to strengthen a weak interaction with the 5-HT_{2A}i3 construct, which had been minimal in the absence of added nucleotide (Fig. 5D). GTPγS did not facilitate T31N-ARF1-HA binding to the receptor constructs. Similar results were obtained in three different experiments.

Further to this work, a range of concentrations of both ARF1 and ARF6 were added to the GST-5-HT_{2A}i3 and GST-5-HT_{2A}ct constructs to assess the concentration-dependence of binding. Figure 6 shows the relative proportion of ARF isoform bound to the constructs at increasing ARF concentrations, expressed as a ratio of densitometric values for HA-immunoreactivity of the bound ARF versus GST immu-

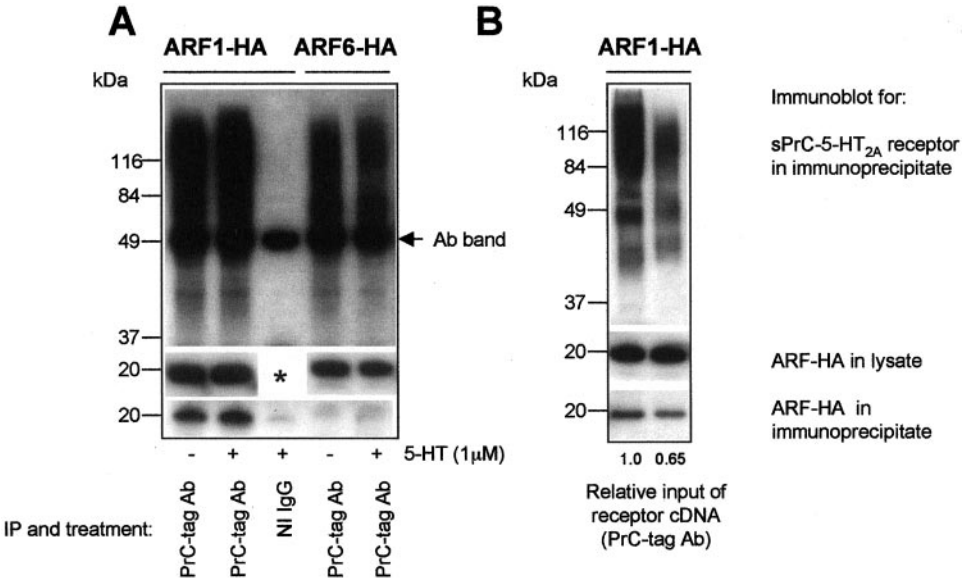

Fig. 2. ARF1-HA and ARF6-HA coimmunoprecipitation with the sPrC-5-HT_{2A} receptor. COS-7 cells were cotransfected with sPrC-5-HT_{2A}R and ARF1-HA or ARF6-HA. A and B, ARF1-HA and ARF6-HA capture in pulldown assays of the sPrC-5-HT_{2A}R carried out with PrC-tag antibody compared with a control procedure using NI IgG. In each case, at the top (anti-PrC-tag immunoblot on immunoprecipitates) are shown pulldown assays of receptor (diffuse bands caused by glycosylation), in which receptor was only detected when immunoprecipitated by PrC-tag antibody, not by NI IgG. The middle (anti-HA immunoblot on sample input) shows that ARF1-HA and ARF6-HA were expressed at similar levels in the compared samples. In A, the ARF input level for lane 3 (NI IgG control), designated by *, was the same as that for lane 2 because the same lysate was split between the two treatments with PrC-tag antibody or nonimmune IgG. The bottom (anti-HA immunoblot on immunoprecipitates) shows specific coimmunoprecipitation of ARF1-HA (or ARF6-HA) with the receptor. A low level of nonspecific pulldown of ARF can be seen in the NI IgG lane. In A, cells were challenged with either 5-HT (1 μM) for 5 min or control. Much more ARF1-HA was pulled down compared with ARF6-HA, even though there was only a small difference in the relative amount of these isoforms expressed in the total lysate. Addition of 5-HT seemed to cause increased coimmunoprecipitation of both isoforms, but the extent of this increase was greater for ARF1-HA. B, the effect of different levels of sPrC-5-HT_{2A}R expression on ARF1-HA coimmunoprecipitation. Cells were transfected with different amounts of expression plasmid for the sPrC-5-HT_{2A}R, with substitution by pcDNA3 vector, thus keeping ARF1-HA expression constant. Cells used for the blot in lane 1 had the standard level of receptor cDNA, whereas cells in lane 2 received 65% of this level. Densitometric analysis indicated that the amount of receptor immunoprecipitated in lane 2 was 71% of that in lane 1 and the amount of ARF1-HA coimmunoprecipitated was 62% of that in lane 1, although the ARF1-HA input level was similar in both samples. In equivalent aliquots of membrane preparations from these cells transfected with the standard or reduced (65%) amount of sPrC-5-HT_{2A}R plasmid, specific [^{3}H]ketanserin binding represented 627 ± 53 and 344 ± 41 dpm per assay, respectively (means ± S.E.M., n = 4).

noreactivity in the construct. Increasing the concentration of ARF1-HA present with each construct caused corresponding increases in the amount of ARF bound. ARF1-HA bound to the GST-5-HT$_{2A}$ct construct to a much greater extent than to the GST-5-HT$_{2A}$i3 construct. ARF6-HA also bound to both the GST-5-HT$_{2A}$ct and the GST-5-HT$_{2A}$i3 constructs, but to a much lesser extent than the ARF1-HA bound to either construct, requiring higher levels of added ARF6-HA to obtain detectable binding. To obtain an estimate of the affinity of ARF1-V5-His$_6$ (added in cytosolic extracts) for the GST-5-HT$_{2A}$ ct construct, we quantified the amount of ARF binding by comparison of densitometric values for V5-immunoreactivity with a coprocessed standard curve of known amounts of ARF1-V5-His$_6$ that had been purified by Co^{2+} affinity column (as above). The ARF-V5-His$_6$ ligand was provided for the interaction assay as an enriched cytosolic extract rather than affinity-purified material because binding was more robust and consistent using this approach. It is not clear whether this is a result of deleterious effects of the purification on ARF1-V5-His$_6$ conformation and function or whether unknown cytosolic factors are additionally required for optimal ARF binding. Working within the linear range of the standard curve for V5-immunoreactive band density against purified ARF1-V5-His$_6$ concentration, we added a range of cytosolic ARF1-V5-His$_6$ concentrations (1–25 ng) to interaction assays and derived values for the amounts of ligand bound from the corresponding V5-immunoreactive band densities. Nonlinear curve fitting of the saturation curve gave a value for affinity (50% saturation) of 1.7 ± 0.4 nM, with greater than 90% occupancy of available sites by 4 to 5 nM.

The differential signaling properties of the wild-type 5-HT$_{2A}$R and the N376D mutant 5-HT$_{2A}$R (Mitchell et al., 1998, 2003) suggest that the NPxxY motif, at the junction of the ct and the 7th transmembrane domain, may participate in the binding of ARF1 to the receptor. To test this theory, we carried out signaling experiments, coimmunoprecipitation, and GST-fusion protein studies with both the wild-type and N376D mutant form of the receptor. Figure 7A shows that 1 μM 5-HT-induced PLD activation by the wild-type sPrC-5-HT$_{2A}$R was significantly reduced by BFA (100 μM) or by coexpression of T31N-ARF1-HA but not T27N-ARF6-HA. Corresponding responses of the N376D-sPrC-5-HT$_{2A}$R examined in the same experiments showed no significant inhibi-

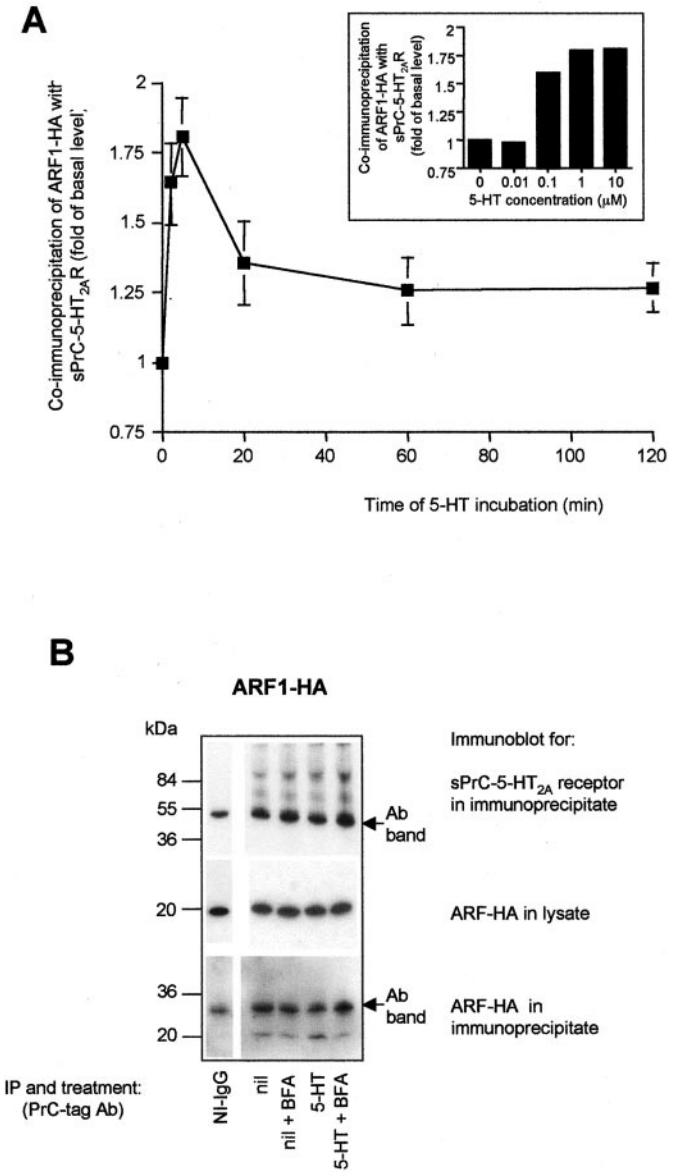

Fig. 3. Characterization of ARF1-HA association with the sPrC-5-HT$_{2A}$ receptor. A, incubation of cells with 5-HT caused a time- and concentration-dependent increase in the amount of ARF1-HA coimmunoprecipitating with the sPrC-5-HT$_{2A}$R. The main figure shows that incubation with 5-HT (1 μM) caused a rapid rise in the association of ARF1-HA to 1.81 ± 0.14 of basal at 5 min, reducing thereafter. Values are means ± S.E.M., n = 4 to 6 at each point. Inset, a single experiment showing a concentration-response curve to 5-HT (10 min) in which a maximal response was reached by 1 μM. This experiment was repeated twice more with similar results. B, effects of BFA on the levels of ARF1-HA associating with the receptor under basal and 5-HT-stimulated conditions. The first lane shows a control immunoprecipitation procedure with nonimmune mouse IgG (NI IgG) instead of the PrC-tag antibody, which was used in all other lanes: nil, no stimulation; nil + BFA, BFA (100 μM, 20 min); 5-HT, 5-HT (10 μM, 10 min); and 5-HT+ BFA, BFA 10 min, followed by 5-HT plus BFA for a further 10 min. Pulldown of receptor (reprobed with the PrC-tag antibody) is shown in the top, input of ARF1-HA in the lysate is shown in the middle, and coimmunoprecipitation of ARF1-HA in PrC-tag antibody-directed pulldown assays is shown in the bottom. Because in these experiments captured proteins were solubilized directly in Laemmli buffer, nonspecific bands can be seen, reflecting the presence of the antibody or control immunoglobulin used for pulldown assays.

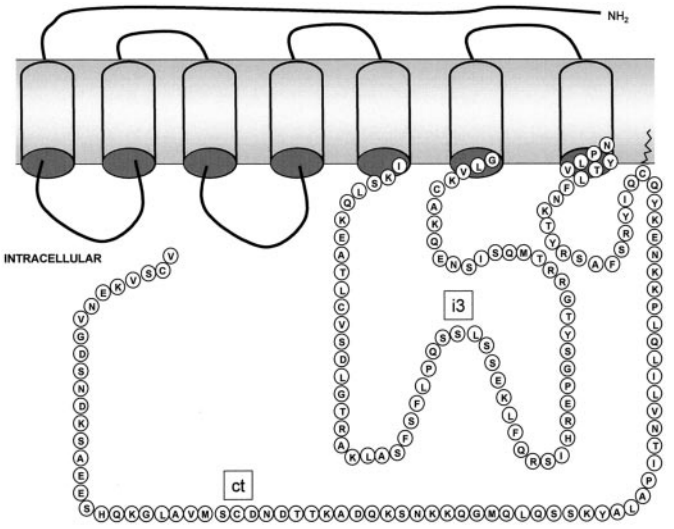

Fig. 4. Amino acid sequences of the 5-HT$_{2A}$ receptor third intracellular loop (i3) and carboxy-terminal (ct) tail inserts incorporated into GST-fusion proteins.

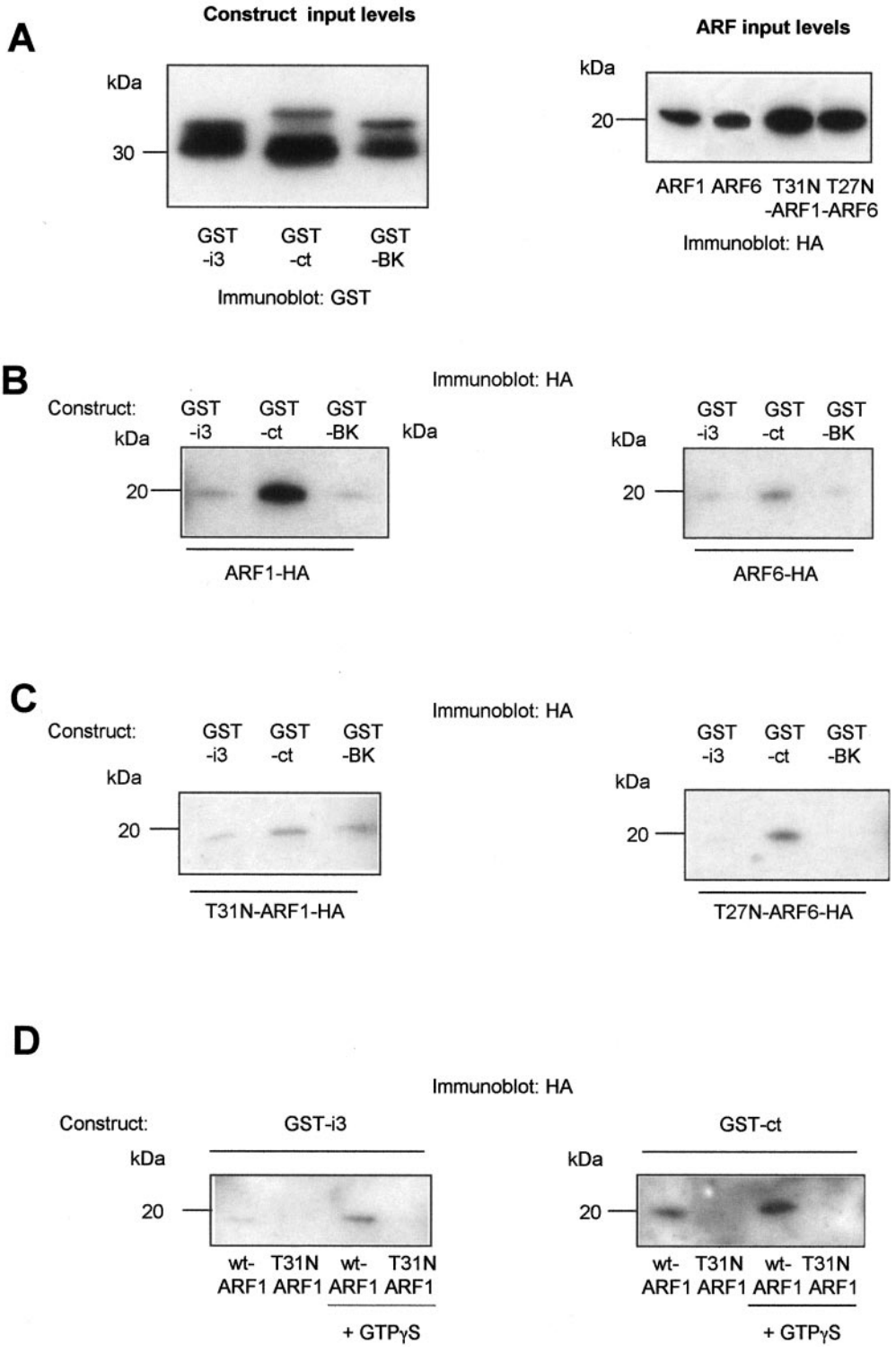

Fig. 5. Interactions of ARF isoforms with GST fusion proteins of domains from the 5-HT_{2A} receptor. GST-5-HT_{2A}i3, GST-5-HT_{2A}ct, and (control) GST-BK channel (STREX exon) constructs were incubated with cellular extracts enriched in particular HA-tagged ARF isoforms. A, input levels of fusion protein constructs and ARF isoforms were balanced in terms of GST immunoreactivity and HA-immunoreactivity, respectively. The fusion protein construct input levels are shown for GST-5-HT_{2A}i3 (GST-i3), GST-5-HT_{2A}ct (GST-ct), and GST-BK running at apparent molecular masses of approximately 36, 40, and 34 kDa, respectively. Unconjugated GST ran at approximately 29 kDa. The ARF input levels are shown for ARF1-HA, ARF6-HA, T31N-ARF1-HA, and T27N-ARF6-HA. B and C, association of the indicated ARF form with GST-5-HT_{2A}i3, GST-5-HT_{2A}ct, and GST-BK constructs, respectively. ARF1-HA bound selectively to the GST-5-HT_{2A}ct construct, with little binding to the GST-5-HT_{2A}i3, or GST-BK constructs. ARF6-HA showed a similar profile but bound to a much lesser extent than ARF1-HA. The T31N mutation in ARF1-HA severely reduced the ability of the protein to bind to the GST-5-HT_{2A}ct construct, but the equivalent mutation in ARF6-HA had no discernible effect. In D, GST-5-HT_{2A}i3 and GST-5-HT_{2A}ct constructs were incubated with cellular extracts enriched in the indicated HA-tagged ARF isoforms in the presence or absence of GTPγS (100 μM). GTPγS increased the binding of wild-type ARF1-HA to both GST-5-HT_{2A}i3 and GST-5-HT_{2A}ct constructs, but did not alter the lack of binding seen with T31N-ARF1-HA.

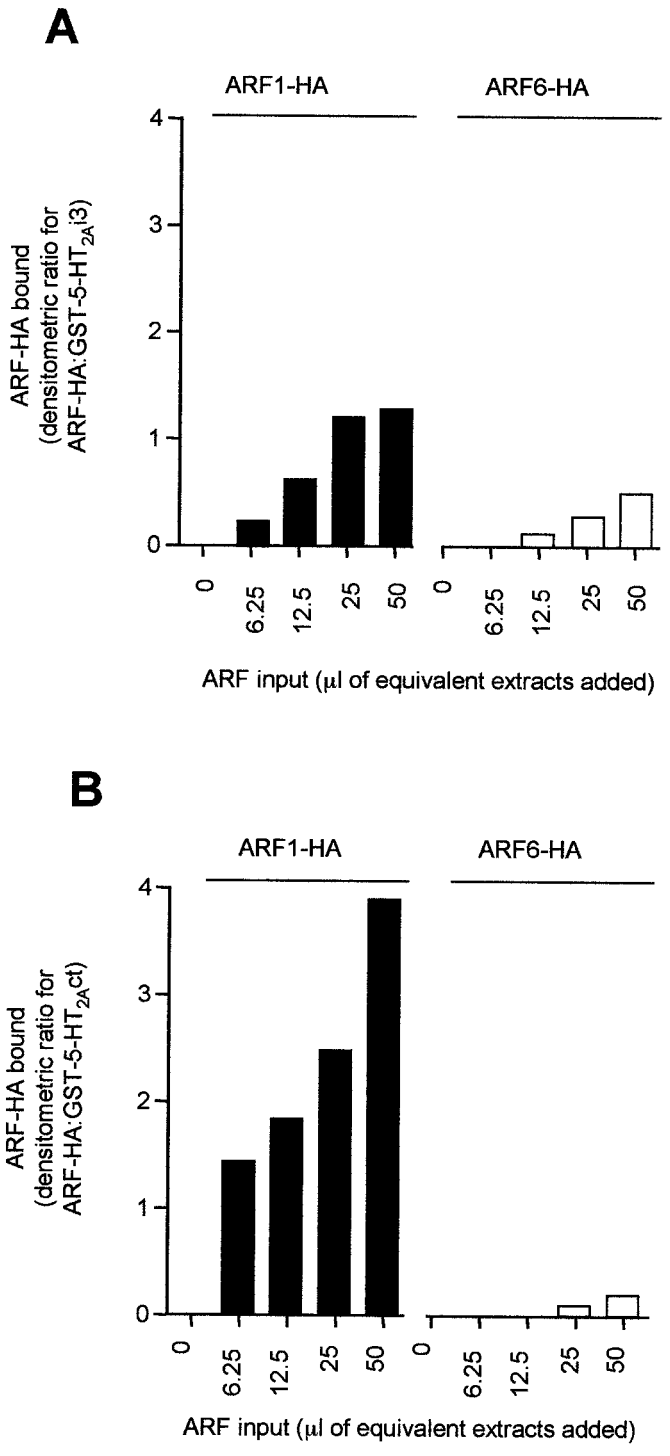

Fig. 6. Concentration-dependence of ARF1-HA and ARF6-HA binding to the GST fusion proteins of domains from the 5-HT$_{2A}$ receptor. GST-5-HT$_{2A}$i3 and GST-5-HT$_{2A}$ct constructs were exposed to increasing amounts of cellular extracts containing ARF1-HA and ARF6-HA. The content of HA-immunoreactive ARF per microliter of the ARF1-HA and ARF6-HA extracts was shown to be equivalent. A, binding of ARF1-HA and ARF6-HA to the GST-5-HT$_{2A}$i3 construct. ARF1-HA bound to the construct in a concentration-dependent manner, as did ARF6, but to a much lesser extent. B, binding of ARF1-HA and ARF6-HA to the GST-5-HT$_{2A}$ct construct. ARF1-HA bound in a concentration-dependent manner, whereas the binding of ARF6-HA was minimal and detectable only at the highest levels of ARF6-HA input.

tion. Figure 7B shows the results of coimmunoprecipitation experiments in COS-7 cells cotransfected with ARF1-HA and either the wild-type sPrC-5-HT$_{2A}$R or its N376D mutant form. After stimulation with 5-HT (1 μM, 5 min) or control, solubilized extracts were immunoprecipitated with HA-tagged antibody, and 5-HT$_{2A}$Rs associated with the immunoprecipitate were assayed as specific [^{3}H]ketanserin binding. Low levels of nonspecific [^{3}H]ketanserin binding were present in each case, and these showed no discernible differences between samples. In cells transfected with the wild-type sPrC-5-HT$_{2A}$R but not those expressing the N376D mutant, significant levels of specific [^{3}H]ketanserin binding became associated with the HA tag immunoprecipitate after 5-HT stimulation. When NI IgG was substituted for the HA tag antibody during immunoprecipitation, no specific [^{3}H]ketanserin binding was captured. Using the [^{3}H]ketanserin binding protocol there was no evidence for significant basal association between ARF1-HA and sPrC-5-HT$_{2A}$R (6 $\pm$ 8% of specific binding), unlike the data shown in Figs. 2 and 3. There were a number of methodological differences (such as shorter time for immunoprecipitation and the addition of glycerol) between this procedure and that used previously, which may result in the differences in basal association. 5-HT stimulation clearly caused an increased interaction between the sPrC-5-HT$_{2A}$R and ARF1-HA. Comparison of the amount of specific [^{3}H]ketanserin binding associated with ARF1-HA immunoprecipitates and the input levels of binding in solubilized extracts gave an estimate that 30 $\pm$ 5% of sPrC-5-HT$_{2a}$Rs were associated with ARF1-HA after 5-HT stimulation. This value is in reasonably close agreement with values estimated from the immunoprecipitation/immunoblot experiments (above).

Figure 7C shows an experiment to investigate whether the N376PLVY motif in the 5-HT$_{2A}$R ct domain may form part of the binding site for ARF1-HA. GST-fusion protein constructs of the wild type (Asn376-Val471) 5-HT$_{2A}$ct, the mutant (N376D-Val471) 5-HT$_{2A}$ct and the truncated (Lys385-Val471) 5-HT$_{2A}$ct were prepared. Equal amounts of these constructs (and GST alone) were determined by Coomassie blue staining and by GST immunoreactivity at the predicted molecular mass before interaction assays with ARF1-HA. The ratios of the densitometric values for bound ARF1-HA immunoreactivity to fusion protein input were then calculated on an arbitrary scale relative to that for the wild-type construct. Both individual images and the mean densitometry ratios for bound ARF1-HA:construct input showed a clear reduction in binding (to around 40% of wild type) by the N376D mutation and a further loss (to around 20%) by deletion of the Asn376-Asn384 sequence (Fig. 7C).

Discussion

The present findings demonstrate that a negative mutant construct of ARF1, but not ARF6, inhibits the activation of PLD, but not PLC, by the 5-HT$_{2A}$R. This indicates a selective functional role for the ARF1 isoform in the PLD signaling pathway of the 5-HT$_{2A}$R. PLD but not PLC responses of the 5-HT$_{2A}$R were correspondingly reduced in a concentration-dependent manner by BFA, an inhibitor of the ARF-GEFs, BIG1/2, which are reported to show selectivity for ARF1 rather than ARF6 (Morinaga et al., 1999). Further evidence consistent with a functional role for ARF1 in BFA-sensitive

PLD responses came from experiments assessing the BFA sensitivity of 5-HT_{2A}R PLD responses in cells coexpressing negative-mutant ARFs, T31N-ARF1-HA or T27N-ARF6-HA. The inhibitory effect of the negative-mutant ARF1 construct pre-empted any further inhibition by BFA, suggesting that they both acted within the same pathway, whereas negative mutant ARF6 was without effect. Other GPCRs may show different selectivity for ARF isoforms. In COS-7 cells express-

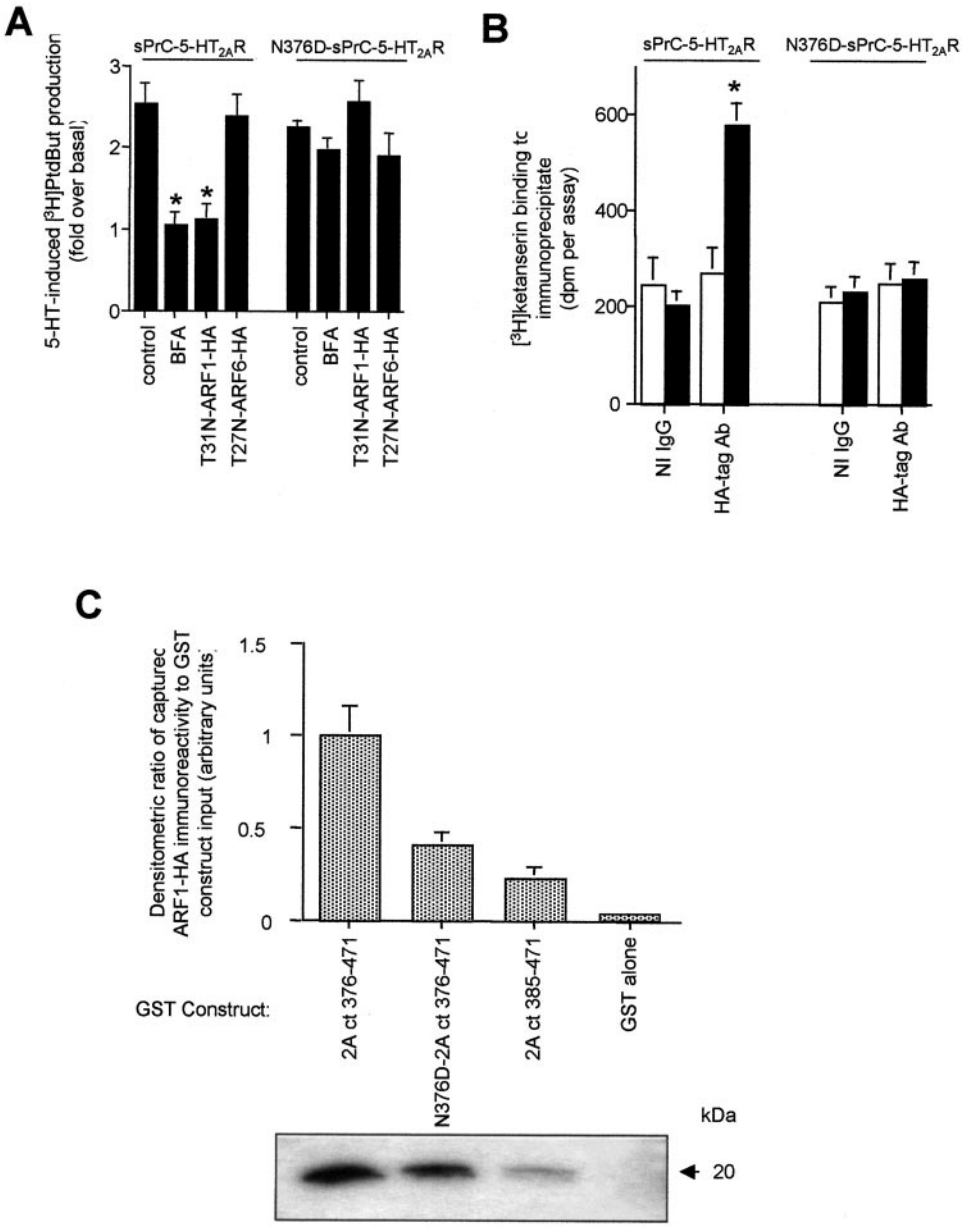

Fig. 7. Interactions of ARF isoforms with wild-type and N376D mutant sPrC-5-HT_{2A} receptors. A, 1 μM 5-HT-induced PLD signaling responses of wild-type and N376D mutant sPrC-5-HT_{2A}R. Comparison of their susceptibility to inhibition by BFA (100 μM) or negative mutant forms of ARF1 (T31N-ARF1) or ARF6 (T27N-ARF6). In control and BFA-treated cells, an amount of empty vector equivalent to that used for the mutant ARFs was cotransfected with the receptor constructs. Values are means ± S.E.M., $n = 6$, *$p < 0.05$ by Wilcoxon test compared with control (5-HT alone). BFA and T31N-ARF1-HA significantly reduced responses of the wild type, but the T27N-ARF6-HA construct had no detectable effect. B, amount of [^{3}H]ketanserin binding to HA-tag directed immunoprecipitates in cells cotransfected with ARF1-HA and either wild-type or N376D mutant sPrC-5-HT_{2A}R. Nonspecific binding of [^{3}H]ketanserin in the presence of 10 μM mianserin fell in the range of 163 to 241 dpm/assay in all cases and showed no discernible difference between samples. Control procedures were carried out with an equivalent amount of nonimmune mouse IgG (NI IgG). Cells were pretreated with 5-HT (1 μM, 5 min, ■) or control (□). Values are means ± S.E.M., $n = 5$, *, $p < 0.05$ by Mann-Whitney U test compared with corresponding HA-immunoprecipitate without 5-HT prestimulation and to control immunoprecipitation with NI IgG. Significant levels of specific [^{3}H]ketanserin binding (above nonspecific binding) were recovered only in HA-tag directed immunoprecipitates from cells in which the wild-type sPrC-5-HT_{2A}R had been prestimulated with 5-HT. The input levels of specific [^{3}H]ketanserin binding in solubilized extracts immediately before immunoprecipitation were similar for the wild-type and N376D mutant receptors (1166 ± 154 and 1450 ± 125 dpm per sample, respectively). C, matched levels of GST-fusion proteins incorporating the (Asn376–Val471) wild-type 5-HT_{2A} receptor ct domain, the corresponding N376D mutant, or a truncated Lys385–Val471 sequence, as well as GST alone, were attached to glutathione-Sepharose beads and incubated with equivalent levels of ARF1-HA. Immunoreactivity for bound ARF1-HA was quantified by densitometry and the ratio to the level of input for each GST-fusion protein construct was calculated. These ratios were then normalized to that found for the wild-type ct construct. Values are means ± S.E.M., $n = 5$. A typical example of ECL film images for HA-immunoreactivity bound to these constructs is shown at bottom.

ing the M_3 muscarinic receptor and in A10 smooth muscle cells, PLD responses to carbachol and to angiotensin II or ET-1, respectively were attenuated by T31N-ARF1 and by T27N-ARF6 (Shome et al., 2000; Mitchell et al., 2003), whereas some other GPCRs such as P_{2u} and $PAC_{1\text{-}hop1}$ receptors may show selectivity for ARF6 over ARF1 (Ronaldson et al., 2002; Mitchell et al., 2003).

Coimmunoprecipitation experiments demonstrated that the sPrC-5-HT$_{2A}$R, under basal conditions, could specifically bind ARF1-HA and to a lesser extent ARF6-HA. The binding of ARF1-HA was increased by 5-HT stimulation of the receptor in a concentration- and time-dependent manner. Only minor increases in the association of ARF6-HA with the sPrC-5-HT$_{2A}$R could be seen. The presence of BFA during the stimulation with 5-HT reversed the 5-HT–induced association of ARF1-HA, although we know from confocal immunofluorescence imaging that BFA does not prevent agonist-induced translocation of ARF1-HA to the plasma membrane (data not shown). This evidence that ARF1 is the isoform predominantly docking to the receptor in a BFA-sensitive manner is consistent with the data on PLD activation. Estimates of the proportion of 5-HT$_{2A}$ receptors that was associated with ARF1-HA after 5-HT stimulation ranged between 30 and 37% depending on the approach taken, with corresponding estimates of basal association between 6 and 23%. Interaction of other proteins, such as $G_{q/11}$ and perhaps arrestins, with the 5-HT$_{2A}$R may well mean that relevant binding sites were not accessible to ARF1 in part of the receptor population.

The GST-fusion protein experiments suggested that the ct domain of the 5-HT$_{2A}$R provides a binding site for ARFs at which ARF1 shows a higher affinity than ARF6. Comparison of the immunoreactivity for ARF1-V5-His$_6$ bound to the GST-5-HT$_{2A}$ct construct with known amounts of purified ARF1-V5-His$_6$ allowed an estimate of the affinity of interaction. This was in the low nanomolar range (1.7 $\pm$ 0.4 nM), which is of lower affinity than that for arrestin interaction with the M_3R i3 domain (Wu et al., 1997) but higher than the corresponding interaction of G$\beta\gamma$ (Wu et al., 1998). The 5-HT$_{2A}$ receptor i3 domain shows only low affinity for ARF in vitro but may still represent an auxiliary binding site in vivo. In contrast, the i3 domain effectively binds arrestins in similar experiments (Gelber et al., 1999). The interaction of ARF1-HA with the ct or i3 domain of the 5-HT$_{2A}$R seemed to be facilitated by GTPγS, suggesting that occupancy of its nucleotide recognition site by GTP rather than GDP promotes the interaction. Correspondingly, the GTP-binding-defective mutant ARF1 construct (T31N-ARF1-HA) showed an almost complete lack of specific binding to the ct or i3 domain GST fusion proteins that was unmodified by GTPγS. The lower level of ARF6-HA binding seemed to be little affected by T27N mutation of ARF6-HA, but this was not investigated further. The means by which agonist induces increased (BFA-sensitive and GTP status-sensitive) binding of ARF1 to the 5-HT$_{2A}$R is not clear. Involvement of BIG1/2 is implicated by the BFA sensitivity, but it is not known whether agonist activation of the receptor might facilitate GTP loading of ARF1 by direct protein-protein interaction, by regulation of BIG1/2, or by other means. However, GTP binding operates a conformational switch in ARFs that might contribute to additional protein-protein interactions (Goldberg, 1998).

Although the tm7 NPxxY motif has been implicated as a critical determinant of ARF coimmunoprecipitation and ARF-dependent signaling in rhodopsin family GPCRs, the precise site of ARF binding to the ct of the 5-HT$_{2A}$R remains to be elucidated. Mutation of this motif to DPxxY strongly inhibits BFA-sensitive, ARF-mediated activation of PLD (Fig. 7A; Mitchell et al., 1998) and sPrC-5-HT$_{2A}$R coimmunoprecipitation with ARF1-HA (Fig. 7B). Using GST-fusion proteins of the 5-HT$_{2A}$R ct domain, mutation of Asn376 to Asp causes a marked (60%) reduction in ARF1-HA association and removal of the Asn376–Asn384 segment reduces association further to around 20% of the wild-type values. This suggests that the majority of the key elements involved in 5-HT$_{2A}$R-ARF1 interaction, at least under these circumstances, may lie within the Asn376–Asn384 segment. Structural modeling based on rhodopsin and secondary structure predictions (PHD predict; http://cubic.bioc.columbia.edu/predictprotein/) suggest that the Pro377 residue is likely to form a pronounced kink in the tm7 helix and that Thr381–Lys385 may form a flexible hinge to an eighth helical segment that runs in the plane of the membrane until a palmitoylation anchor at Cys397 (Konvicka et al., 1998; Palczewski et al., 2000; Yeagle et al., 2000; Visiers et al., 2002). In the case of rhodopsin, activation of the receptor newly exposes to the intracellular surface an epitope that includes residues equivalent to Leu378–Tyr380 here (Abdulaev and Ridge, 1998), consistent with the idea that receptor activation may reveal residues involved in ARF association. The predicted fourth intracellular loop of rhodopsin, in particular residues equivalent to Asn384–Gln386 here, is involved in interaction with the α and γ subunits of transducin (Ernst et al., 2000; Marin et al., 2000). Interactions between amino acids in the NPxxY motif and the subsequent seven residues are thought to influence heterotrimeric G protein activation by both rhodopsin and the 5-HT$_{2C}$R (Prioleau et al., 2002; Fritze et al., 2003). Elements of this surface might also contribute to ARF docking. The interaction of 5-HT$_{2A}$R with G$\alpha_{q/11}$, however, is also thought to involve the carboxyl portion of the i3 loop (Roth et al., 1998).

Additional functional roles have been proposed for the N/DPxxY motif. The most consistent evidence is for a role linking the tm2 and tm7 helices (Sealfon et al., 1995). The NPxxY motif and the Y residue in particular have been proposed to constitute an internalization motif in some but by no means all GPCRs (Hunyady et al., 1995). Mutation of the Asn or Asp residue to Ala generally causes massive disruption of signaling pathways and of internalization, whereas reciprocal mutation of Asn or Asp seems to have relatively minor effects other than on ARF-dependent PLD activation (Sealfon et al., 1995; Le Gouill et al., 1997; Mitchell et al., 1998). In the case of the 5-HT$_{2A}$ receptor, we confirmed that the NPxxY motif, rather than the DPxxY mutant motif, was necessary for functional BFA-sensitive and T31N-ARF1-HA-sensitive PLD responses from the receptor for 5-HT-induced coimmunoprecipitation of the receptor with ARF1-HA and for the major part of in vitro binding of ARF1-HA to the ct domain of the receptor.

There is increasing evidence that particular GPCRs can interact with diverse scaffolding and signaling proteins other than their conventional partners, the heterotrimeric G-proteins (Brady and Limbird, 2002; Premont and Hall, 2002). Receptor ct segments may dock bivalent adapter proteins containing PDZ or other domains, signaling proteins, and modulators of signaling functions (Dev et al., 2001; Oakley et

al., 2001; Brady and Limbird, 2002). In the 5-HT_2 receptor family, the distal ct residues are targeted by the PDZ-domain proteins PSD-95 and MUPP-1 (Backstrom et al., 2000; Becamel et al., 2001; Xia et al., 2003), interactions that may modify the signaling function of the receptors. A novel PDZ domain protein, tamalin, has been shown to bind to both mGluR1/5 receptors and the ARF-GEF ARNO (Kitano et al., 2002). It is conceivable that an analogous arrangement might occur in the case of the 5-HT_{2A} receptor, locating an ARF-GEF in the proximity of ARF.

ARF may not be the only small G protein that can interact with GPCRs. We showed that Rho A can be coimmunoprecipitated in a complex with NPxxY GPCRs (Mitchell et al., 1998), and there is evidence that both $G\alpha_{13}$ and $G\alpha_q$ may interact with Rho-GEFs to facilitate Rho function (Sagi et al., 2001). Other small G proteins of unknown identity have also been found to associate with the formyl-Met-Leu-Phe receptor (Polakis et al., 1989).

In summary, these experiments provide intracellular signaling, coimmunoprecipitation and in vitro domain interaction evidence for ARF association with the 5-HT_{2A}R, corresponding to its functional activation of PLD. Furthermore, ARF1 rather than ARF6 seems to participate in this mechanism through GTP-dependent interaction with a ct domain of the receptor.

Acknowledgments

We are grateful to Stuart Sealfon and Julie Donaldson for their kind gifts of reagents.

References

Abdulaev NG and Ridge KD (1998) Light-induced exposure of the cytoplasmic end of transmembrane helix seven in rhodopsin. *Proc Natl Acad Sci USA* **95:**12854–12859.

Backstrom JR, Price RD, Reasoner DT, and Sanders-Bush E (2000) Deletion of the serotonin 5-HT2C receptor PDZ recognition motif prevents receptor phosphorylation and delays resensitization of receptor responses. *J Biol Chem* **275:**23620–23626.

Becamel C, Figge A, Poliak S, Dumuis A, Peles E, Bockaert J, Lubbert H, and Ullmer C (2001) Interaction of serotonin 5-hydroxytryptamine type 2C receptors with PDZ10 of the multi-PDZ domain protein MUPP1. *J Biol Chem* **276:**12974–12982.

Berg KA, Maayani S, Goldfarb J, Scaramellini C, Leff P, and Clarke WP (1998) Effector pathway-dependent relative efficacy at serotonin type 2A and 2C receptors: evidence for agonist-directed trafficking of receptor stimulus. *Mol Pharmacol* **54:**94–104.

Brady AE and Limbird LE (2002) G protein-coupled receptor interacting proteins: emerging roles in localization and signal transduction. *Cell Signal* **14:**297–309.

Cavenagh MM, Whitney JA, Carroll K, Zhang C, Boman AL, Rosenwald AG, Mellman I, and Kahn RA (1996) Intracellular distribution of ARF proteins in mammalian cells. ARF6 is uniquely localized to the plasma membrane. *J Biol Chem* **271:**21767–21774.

D'Souza-Schorey C, Li G, Colombo MI, and Stahl PD (1995) A regulatory role for ARF6 in receptor-mediated endocytosis. *Science (Wash DC)* **267:**1175–1178.

Dev KK, Nakanishi S, and Henley JM (2001) Regulation of mglu(7) receptors by proteins that interact with the intracellular C terminus. *Trends Pharmacol Sci* **22:**355–361.

Ernst OP, Meyer CK, Marin EP, Henklein P, Fu WY, Sakmar TP, and Hofmann KP (2000) Mutation of the fourth cytoplasmic loop of rhodopsin affects binding of transducin and peptides derived from the carboxyl-terminal sequences of transducin α and γ subunits. *J Biol Chem* **275:**1937–1943.

Fritze O, Filipek S, Kuksa V, Palczewski K, Hofmann KP, and Ernst OP (2003) Role of the conserved NPxxY(x)5, 6F motif in the rhodopsin ground state and during activation. *Proc Natl Acad Sci USA* **100:**2290–2295.

Gelber EI, Kroeze WK, Willins DL, Gray JA, Sinar CA, Hyde EG, Gurevich V, Benovic J and Roth BL (1999) Structure and function of the third intracellular loop of the 5-hydroxytryptamine2A receptor: the third intracellular loop is alpha-helical and binds purified arrestins. *J Neurochem* **72:**2206–2214.

Goldberg J (1998) Structural basis for activation of ARF GTPase: mechanisms of guanine nucleotide exchange and GTP-myristoyl switching. *Cell* **95:**237–248.

Guillet-Deniau I, Burnol AF, and Girard J (1997) Identification and localization of a skeletal muscle serotonin 5-HT2A receptor coupled to the Jak/STAT pathway. *J Biol Chem* **272:**14825–14829.

Hunyady L, Bor M, Baukal AJ, Balla T, and Catt KJ (1995) A conserved NPLFY sequence contributes to agonist binding and signal transduction but is not an internalization signal for the type 1 angiotensin II receptor. *J Biol Chem* **270:**16602–16609.

Kitano J, Kimura K, Yamazaki Y, Soda T, Shigemoto R, Nakajima Y, and Nakanishi S (2002) Tamalin, a PDZ domain-containing protein, links a protein complex formation of group 1 metabotropic glutamate receptors and the guanine nucleotide exchange factor cytohesins. *J Neurosci* **22:**1280–1289.

Konvicka K, Guarnieri F, Ballesteros JA, and Weinstein H (1998) A proposed structure for transmembrane segment 7 of G protein-coupled receptors incorporating an Asn-Pro/Asp-Pro motif. *Biophys J* **75:**601–611.

Le Gouill C, Parent JL, Rola-Pleszczynski M, and Stankova J (1997) Structural and functional requirements for agonist-induced internalization of the human platelet-activating factor receptor. *J Biol Chem* **272:**21289–21295.

Marin EP, Krishna AG, Zvyaga TA, Isele J, Siebert F, and Sakmar TP (2000) The amino terminus of the fourth cytoplasmic loop of rhodopsin modulates rhodopsin-transducin interaction. *J Biol Chem* **275:**1930–1936.

McCulloch DA, Lutz EM, Johnson MS, Robertson DN, MacKenzie CJ, Holland PJ, and Mitchell R (2001) ADP-ribosylation factor-dependent phospholipase D activation by VPAC receptors and a PAC_1 receptor splice variant. *Mol Pharmacol* **59:**1523–1532.

Mitchell R, McCulloch D, Lutz E, Johnson M, MacKenzie C, Fennell M, Fink G, Zhou W, and Sealfon SC (1998) Rhodopsin-family receptors associate with small G proteins to activate phospholipase D. *Nature (Lond)* **392:**411–414.

Mitchell R, Robertson DN, Holland PJ, Collins D, Lutz EM, and Johnson MS (2003) ADP-ribosylation factor-dependent phospholipase D activation by the M3 muscarinic receptor. *J Biol Chem* **278:**33818–33830.

Morinaga N, Adamik R, Moss J, and Vaughan M (1999) Brefeldin A inhibited activity of the sec7 domain of p200, a mammalian guanine nucleotide-exchange protein for ADP-ribosylation factors. *J Biol Chem* **274:**17417–17423.

Oakley RH, Laporte SA, Holt JA, Barak LS, and Caron MG (2001) Molecular determinants underlying the formation of stable intracellular G protein-coupled receptor-β-arrestin complexes after receptor endocytosis. *J Biol Chem* **276:**19452–19460.

Palczewski K, Kumasaka T, Hori T, Behnke CA, Motoshima H, Fox BA, Le Trong I, Teller DC, Okada T, Stenkamp RE, et al. (2000) Crystal structure of rhodopsin: a G protein-coupled receptor. *Science (Wash DC)* **289:**739–745.

Peters PJ, Hsu VW, Ooi CE, Finazzi D, Teal SB, Oorschot V, Donaldson JG, and Klausner RD (1995) Overexpression of wild-type and mutant ARF1 and ARF6: distinct perturbations of nonoverlapping membrane compartments. *J Cell Biol* **128:**1003–1017.

Polakis PG, Evans T, and Snyderman R (1989) Multiple chromatographic forms of the formylpeptide chemoattractant receptor and their relationship to GTP-binding proteins. *Biochem Biophys Res Commun* **161:**276–283.

Premont RT and Hall RA (2002) Identification of novel G protein-coupled receptor-interacting proteins. *Methods Enzymol* **343:**611–621.

Prioleau C, Visiers I, Ebersole BJ, Weinstein H, and Sealfon SC (2002) Conserved helix 7 tyrosine acts as a multistate conformational switch in the 5HT2C receptor. Identification of a novel "locked-on" phenotype and double revertant mutations. *J Biol Chem* **277:**36577–36584.

Raymond JR, Mukhin YV, Gelasco A, Turner J, Collinsworth G, Gettys TW, Grewal JS, and Garnovskaya MN (2001) Multiplicity of mechanisms of serotonin receptor signal transduction. *Pharmacol Ther* **92:**179–212.

Ronaldson E, Robertson DN, Johnson MS, Holland PJ, Mitchell R, and Lutz EM (2002) Specific interaction between the hop1 intracellular loop 3 domain of the human PAC(1) receptor and ARF. *Regul Pept* **109:**193–198.

Roth BL, Willins DL, Kristiansen K, and Kroeze WK (1998) 5-Hydroxytryptamine2-family receptors (5-hydroxytryptamine2A, 5-hydroxytryptamine2B, 5-hydroxytryptamine2C): where structure meets function. *Pharmacol Ther* **79:**231–257.

Sagi SA, Seasholtz TM, Kobiashvili M, Wilson BA, Toksoz D, and Brown JH (2001) Physical and functional interactions of Gαq with Rho and its exchange factors. *J Biol Chem* **276:**15445–15452.

Sealfon SC, Chi L, Ebersole BJ, Rodic V, Zhang D, Ballesteros JA, and Weinstein H (1995) Related contribution of specific helix 2 and 7 residues to conformational activation of the serotonin 5-HT2A receptor. *J Biol Chem* **270:**16683–16688.

Shome K, Rizzo MA, Vasudevan C, Andresen B, and Romero G (2000) The activation of phospholipase D by endothelin-1, angiotensin II and platelet-derived growth factor in vascular smooth muscle A10 cells is mediated by small G proteins of the ADP-ribosylation factor family. *Endocrinology* **141:**2200–2208.

Visiers I, Ballesteros JA, and Weinstein H (2002) Three-dimensional representations of G protein-coupled receptor structures and mechanisms. *Methods Enzymol* **343:**329–371.

Wess J, Liu J, Blin N, Yun J, Lerche C, and Kostenis E (1997) Structural basis of receptor/G protein coupling selectivity studied with muscarinic receptors as model systems. *Life Sci* **60:**1007–1014.

Wu G, Benovic JL, Hildebrandt JD, and Lanier SM (1998) Receptor docking sites for G-protein $\beta\gamma$ subunits. Implications for signal regulation. *J Biol Chem* **273:**7197–7200.

Wu G, Krupnick JG, Benovic JL, and Lanier SM (1997) Interaction of arrestins with intracellular domains of muscarinic and α2-adrenergic receptors. *J Biol Chem* **272:**17836–17842.

Xia Z, Gray JA, Compton-Toth BA, and Roth BL (2003) A direct interaction of PSD-95 with 5-HT2A serotonin receptors regulates receptor trafficking and signal transduction. *J Biol Chem* **278:**21901–21908.

Yeagle PL, Danis C, Choi G, Alderfer JL, and Albert AD (2000) Three dimensional structure of the seventh transmembrane helical domain of the G-protein receptor, rhodopsin. *Mol Vis* **6:**125–131.

Address correspondence to: Rory Mitchell, MRC Membrane and Adapter Proteins Co-operative Group, Membrane Biology Interdisciplinary Research Group, University of Edinburgh, School of Biomedical and Clinical Laboratory Sciences, Hugh Robson Building, George Square, Edinburgh, Scotland, EH8 9XD, UK. E-mail: rory.mitchell@ed.ac.uk